

Supplemental Information

S1. Rainfall-Runoff Event Detection and Identification (RREDI) Toolkit

The RREDI toolkit was developed to automatically separate rainfall-runoff events for any watershed using time-series signal processing in four steps (Fig. S1) (Canham and Lane, 2022). First, rainfall-runoff event pairs are identified using daily streamflow and precipitation data (step 1) then runoff event start, peak, and end timing are identified using 15-minute streamflow data (step 2). Next, rainfall-runoff event metrics are calculated (step 3) and finally, rainfall-runoff event flagging is performed to remove incorrectly identified rainfall-runoff events (step 4). The RREDI toolkit was fully automated using the open-source python language.

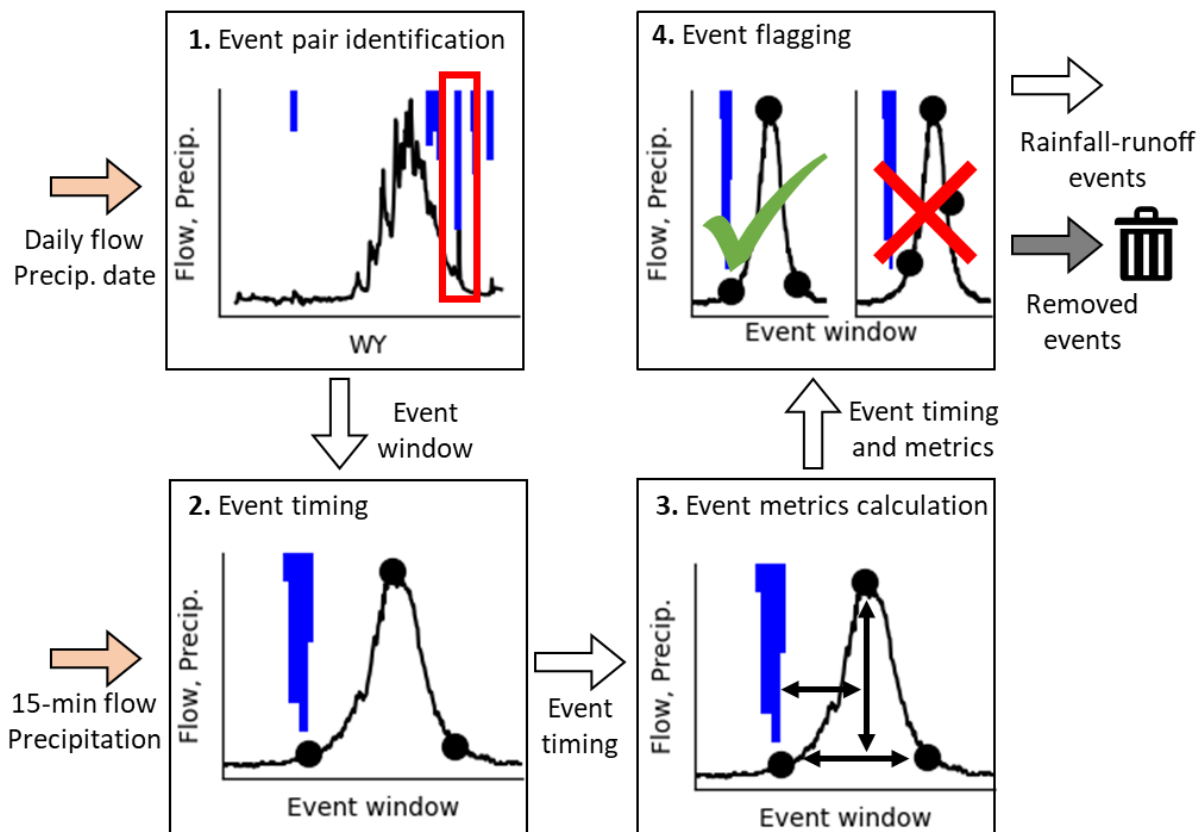


Figure S1: The four key steps for the RREDI toolkit: Step 1. Event pair identification, Step 2. Event timing, Step 3. Event metrics calculation, and Step 4. Event Flagging. Data inputs are shown as orange arrows, removed events are grey arrows, and outputs are white arrows.

Data inputs

Streamflow (daily and 15-minute) and precipitation (sub-daily) data are required inputs to the RREDI toolkit for each study watershed. In this study, streamflow data was obtained from the U.S. Geological Survey's National Water Information System and hourly precipitation timeseries was obtained for the watershed centroid from the Analysis of Record Calibration (AORC) 4km² resolution dataset for water years 1980 to 2022 (Fall et al., 2023). Linear interpolation was then used to develop an instantaneous precipitation record at the AORC resolution of 1 mm by identifying uniform sub-timesteps within the hours timestep resolution. For example, hourly precipitation of 2 mm depth was uniformly spread over the hour with two timesteps of 1 mm each.

Step 1: Rainfall-runoff event pair identification

Rainfall-runoff event pairs were identified based on the co-occurrence of separately identified rainfall and runoff events from the overlapping period of record (Fig. S1, Step 1). Individual rainfall events were identified from the interpolated AORC-based precipitation timeseries over the period of record using a watershed-specific rainfall event gap. First, rainfall events were generated using the interpolated precipitation timeseries and a series of potential rainfall gaps ranging from 0.5 to 24 hours in half hour increments. A curve was then created of the number of rainfall events generated based on each potential rainfall gap (Fig. S2). The precipitation gap was identified as the increment at which the 2nd derivative of the curve decreased below zero. The identified gaps ranged from 4.5 hours for Clear Creek, Arroyo Seco, and Cache La Poudre watersheds to 9 hours for Shitike Creek (Table S1). For each rainfall event, the rainfall duration, cumulative and total depth, intensity, and 60-minute intensity were calculated.

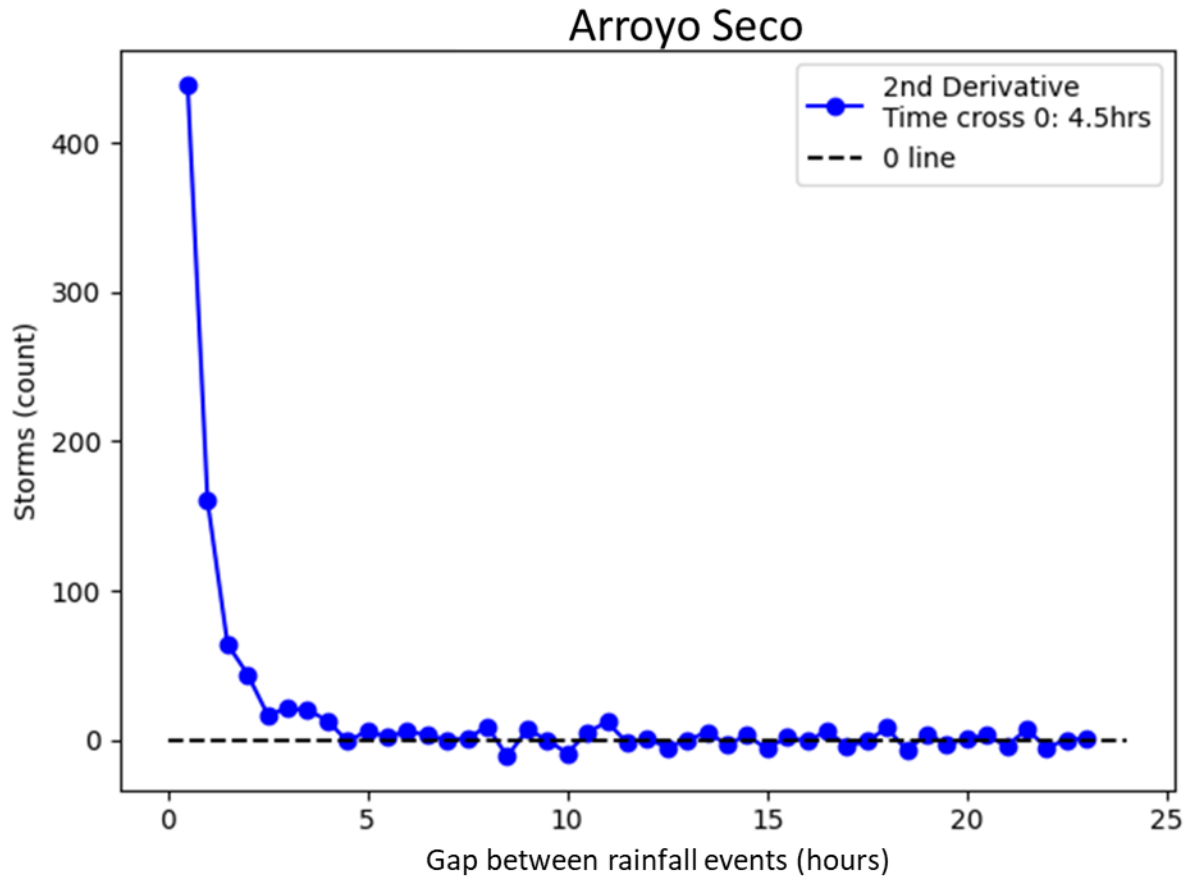


Figure S2: Rainfall event gap identification method. Example from Arroyo Seco. Where the 2nd derivative of the number of rainfall events generated for each of the identified gaps between 0.5 to 24 hours on the half hour is shown (blue). In this example, the identified rainfall gap is 4.5 hours.

Table S1: RREDI toolkit watershed specific parameters

| Watershed | Rainfall event gap (hr) | Stream Classification* |
|-----------------------|-------------------------|------------------------|
| Arroyo Seco | 4.5 | 8 |
| Ash Canyon Creek | 5.5 | 2 |
| Cache La Poudre River | 4.5 | 3 |
| Camp Creek | 6 | 3 |
| Clear Creek | 4.5 | 3 |
| Shitike Creek | 9 | 3 |
| Thompson River | 7 | 2 |
| Valley Creek | 4.5 | 3 |
| Wet Bottom Creek | 7 | 7 |

*Stream classification is divided into nine natural hydrologic classes (Lane et al., 2018) used in streamflow signal processing (Patterson et al., 2020).

To identify runoff events, automated feature detection and signal processing of daily average streamflow data was applied following Patterson et al. (2020). Signal processing theory provided techniques including data smoothing, peak detection, and window processing that were used to automate detection of features from a timeseries. Runoff event features were identified by fitting a gaussian filter and windowing daily streamflow time series. Sign changes in the derivative of a spline curve fit to the filtered streamflow data within each window were used to identify runoff event peaks. The start and end date of the runoff event was then identified using a combination of the relative magnitude and slope of the gaussian filter within the window (Patterson et al., 2020). The parameters for the spline curve and gaussian filter, used across all study watersheds, were manually tuned to identify runoff peaks (Table S2). Finally, to identify rainfall-runoff event pairs, for each rainfall event an associated runoff event was searched for from the rainfall date through the following day. If a runoff event was found within the search window, a rainfall-runoff event pair was returned. If multiple runoff events were associated with a rainfall event, multiple pairs were returned. If no runoff event was found, no rainfall-runoff event pair was returned. For each rainfall-runoff event pair, the event window from the start of rainfall to the end of runoff was passed to step 2.

Table S2: RREDI toolkit calibrated parameters and thresholds

| Parameter | Value |
|--|------------|
| Fall flush gaussian filter sigma (Patterson et al., 2020) (step 1) | 0.05 |
| Fall flush gaussian filter broad sigma (Patterson et al., 2020) (step 1) | 15 |
| Fall flush peak sensitivity (Patterson et al., 2020) (step 1) | 0.05 |
| Start threshold (step 2) | 0.1 |
| End winter threshold (step 2) | 0.25 |
| End melt threshold (step 2) | 0.75 |
| End summer threshold (step 2) | 0.25 |
| End change rate (step 2) | 0 to -0.05 |

Step 2: Rainfall-runoff event timing

For each rainfall-runoff event pair, the start, peak, and end times of each runoff event were identified (Fig. S3 a) using the 15-minute streamflow and precipitation 60-minute intensity (Fig. S1, Step 2). To identify the runoff event peak time, two search windows were used: the during-rainfall event search window between the rainfall start time plus 15 minutes and the rainfall end time, and the after-rainfall search window between the rainfall end time and the rainfall end plus 24 hours. The first 12-hour local maximum extreme value and absolute maximum values were identified in each window. Three sequential comparisons were then completed to identify the runoff peak: (1) the peak was the after-rainfall local 12-hour maximum if it was greater than the during-rainfall absolute maximum, (2) the peak was the during-rainfall absolute maximum if it was greater than the after-rainfall absolute maximum, and (3) the peak was the greater of the after-rainfall absolute maximum and the during-rainfall 12-hour extreme maximum. The search window for the runoff start time was between the rainfall start time plus 15 minutes and the runoff peak time. The runoff start time was when the first derivative of the hourly streamflow timeseries exceeded a threshold of 0.1. If no value exceeded the threshold, the start of the search window was assigned as the rainfall start time. The search window for the runoff end time was between the peak time and the rainfall end plus 24 hours. The end time was set as the first time the hourly streamflow fell below the peak magnitude minus the start magnitude hydrologic season specific threshold (Table S2) and the next occurrence of either a local minimum or when the streamflow first derivative was between 0 and -0.05 and remained negative for the next 5 timesteps. Hourly streamflow was used for the start and end to decrease the noise inherent in the 15-minute streamflow data. All threshold values for runoff event timing identification were determined based on the observation of many runoff events across the nine study watersheds.

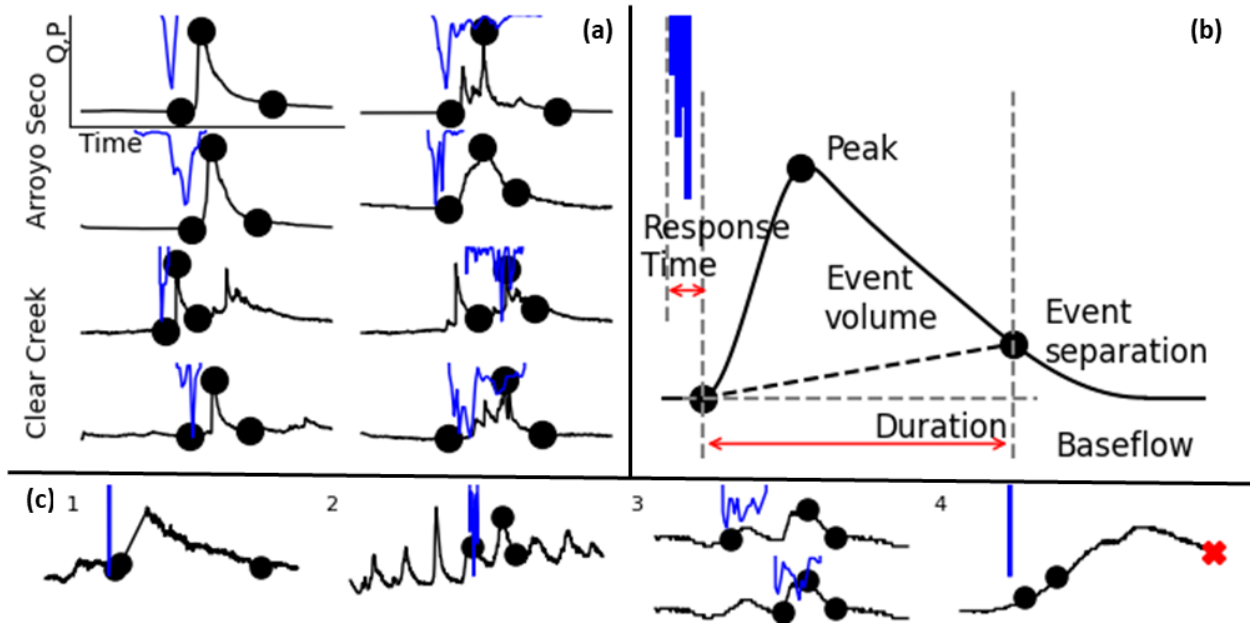


Figure S3: RREDI toolkit rainfall-runoff event examples and metrics. (a) Eight example rainfall-runoff events identified using the RREDI toolkit. Shown are the rainfall event (blue), the paired runoff event hydrograph (black), and the identified runoff start, peak, and end times and magnitudes (black dots). (b) Example rainfall-runoff event showing relevant rainfall-runoff event metrics including rise, peak, runoff event volume, duration, and response time. Runoff event separation (black dashed) between runoff event flow volume and baseflow is shown. (c) Example rainfall-runoff events with issues flagged for removal (Step 4) including (1) missing 15-minute streamflow data, (2) diurnal cycling, (3) duplicate rainfall-runoff events where the top event has the same peak and end time as the bottom event, and (4) no end time found where the defaulted end is marked by a red x.

After the runoff event start, peak, and end times were identified, baseflow was separated from event flow to calculate event volume. Several digital filter baseflow separation methods were evaluated (Chapman and Maxwell, 1996; Eckhardt, 2005), but no identified method could accurately perform baseflow separation at the 15-minute resolution. Instead, linear interpolation between the streamflow magnitudes at the runoff event start and end was applied, resulting in a baseflow separation that closely followed what one would separate manually by visual inspection. For each rainfall-runoff event the start, peak, and end times and magnitudes and the runoff event volume were passed as input to step 3.

Step 3: Rainfall-runoff event metrics calculation

For each rainfall-runoff event a set of 17 metrics (Fig. S4, Table S3) were calculated using the runoff event start, peak, and end timing and magnitudes and runoff event volume (Fig. S1, Step 3). Metrics fell within four runoff metric groups: runoff volume metrics, runoff magnitude metrics, runoff duration metrics, and rainfall-runoff timing metrics. Metrics utilized further in this study included those as follows (Fig. S3 b). The runoff volume metric group included event volume. The runoff magnitude metric group included runoff peak as the peak magnitude. The runoff duration

metric group included event duration calculated as the difference between the runoff event start and end times. The rainfall-runoff timing metric group included response time calculated as the difference between the rainfall start time and the runoff start time. Metrics were also normalized by contributing area to facilitate comparison between study watersheds. The rainfall-runoff event timing and calculated metrics for each rainfall-runoff event were then passed to step 4.

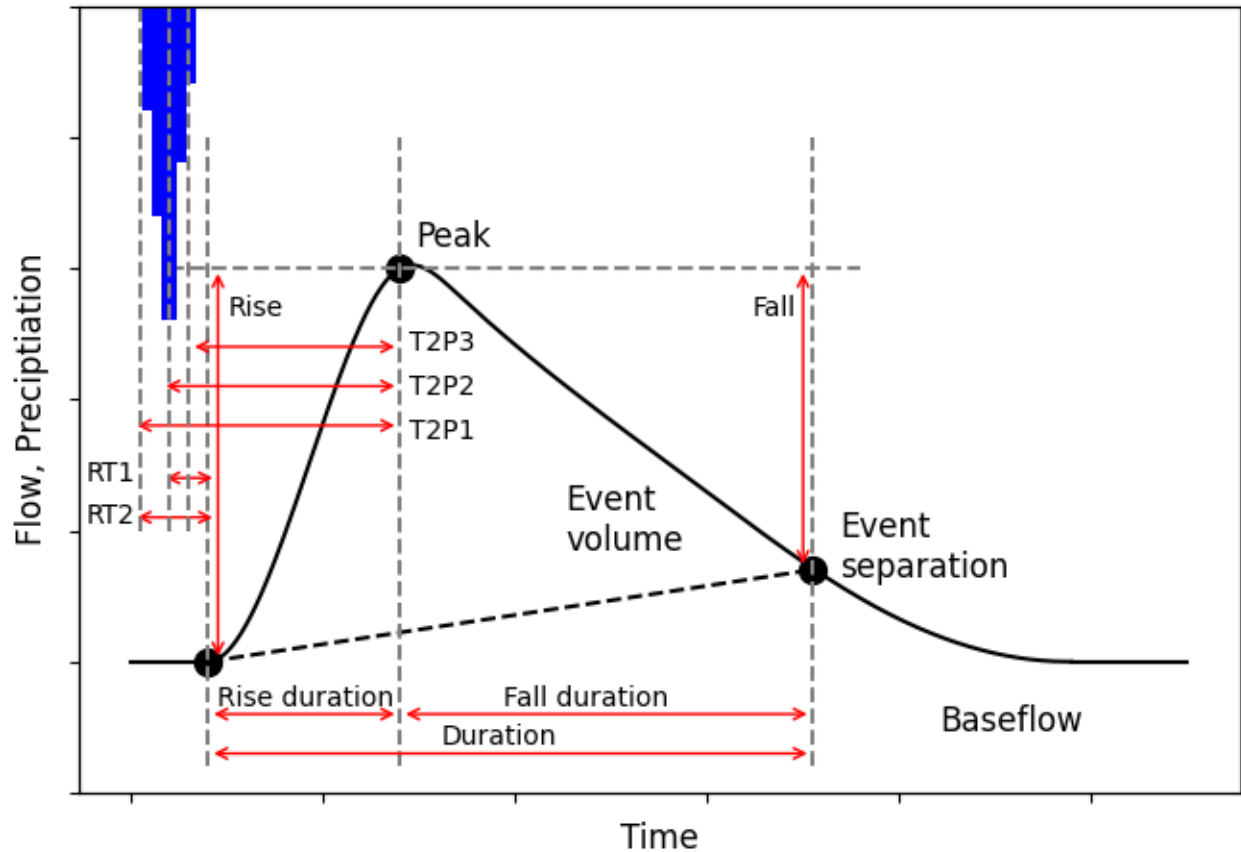


Figure S4: Calculated rainfall-runoff event metrics. Shown is an example rainfall-runoff event with the example hyetograph (blue) and hydrograph (black). The identified runoff start, peak, and end timing are shown consecutively (black dots). Runoff event separation (black dashed) between runoff event flow and baseflow is shown. Event metrics are defined by red arrows and listed in Table S3.

Table S3: RREDI toolkit rainfall-runoff metrics organized by runoff event metric groups. Metric groups include runoff volume metric group, runoff magnitude metric group, runoff duration metric group, and rainfall-runoff timing metric group.

| Runoff volume | Runoff magnitude | Runoff duration | Rainfall-runoff timing |
|-------------------|-------------------------|-----------------------------|------------------------|
| Volume | Peak | Duration | Response time v1 (RT1) |
| Runoff ratio (RR) | Rise | Rise duration (rising_dur) | Response time v2 (RT2) |
| | Fall | Fall duration (falling_dur) | Time to peak v1 (T2P1) |
| | Rise (%) (Rise_percent) | | Time to peak v2 (T2P2) |
| | Fall (%) (Fall_percent) | | Time to peak v3 (T2P3) |
| | Rise rate (RiseRate) | | |
| | Fall rate (FallRate) | | |

Set of equations included within the RREDI toolkit code.

Step 4: Rainfall-runoff event flagging

Four rainfall-runoff event identification issues were systematically flagged for removal: gaps in 15-minute streamflow data, diurnal cycling, duplicate rainfall-runoff events, and no identified runoff event end time (Fig. S1, Step 4). Since streamflow data gaps can cause error in runoff event timing identification, rainfall-runoff events containing any 15-minute data gaps were removed from subsequent analysis (Fig. S3 c 1). Diurnal flow cycling may be caused by snowmelt or water withdrawals (e.g., irrigation diversions) (Fig. S3 c 2). To remove rainfall-runoff events influenced by diurnal flow cycling, we: (1) determined if a rainfall-runoff event fell within a diurnal cycling period and, if so, (2) determined if the rainfall-runoff event was influenced by the diurnal cycling (Fig. S5). A diurnal cycling period was defined as when more than 50% of the daily range (daily maximum minus daily minimum) magnitudes of the four days before and after the rainfall-runoff event occurred within 20% of the mean daily range magnitude. A rainfall-runoff event was considered influenced by diurnal cycling if the runoff event rise was less than three times the mean daily rise. This method was calibrated through visual inspection of many snowmelt- and irrigation-driven runoff events across the study watersheds. Rainfall-runoff events were considered duplicates if the same runoff peak was identified for multiple rainfall events, such as occurred if the first rainfall event generated no distinct runoff response (Fig. S3 c 3). In this case, the rainfall-runoff event pair with the earlier rainfall event was removed. Finally, rainfall-runoff events were removed if no runoff end time was identified that met the established criteria (Fig. S3 c 4). The retained rainfall-runoff events were then output as a rainfall-runoff even dataset.

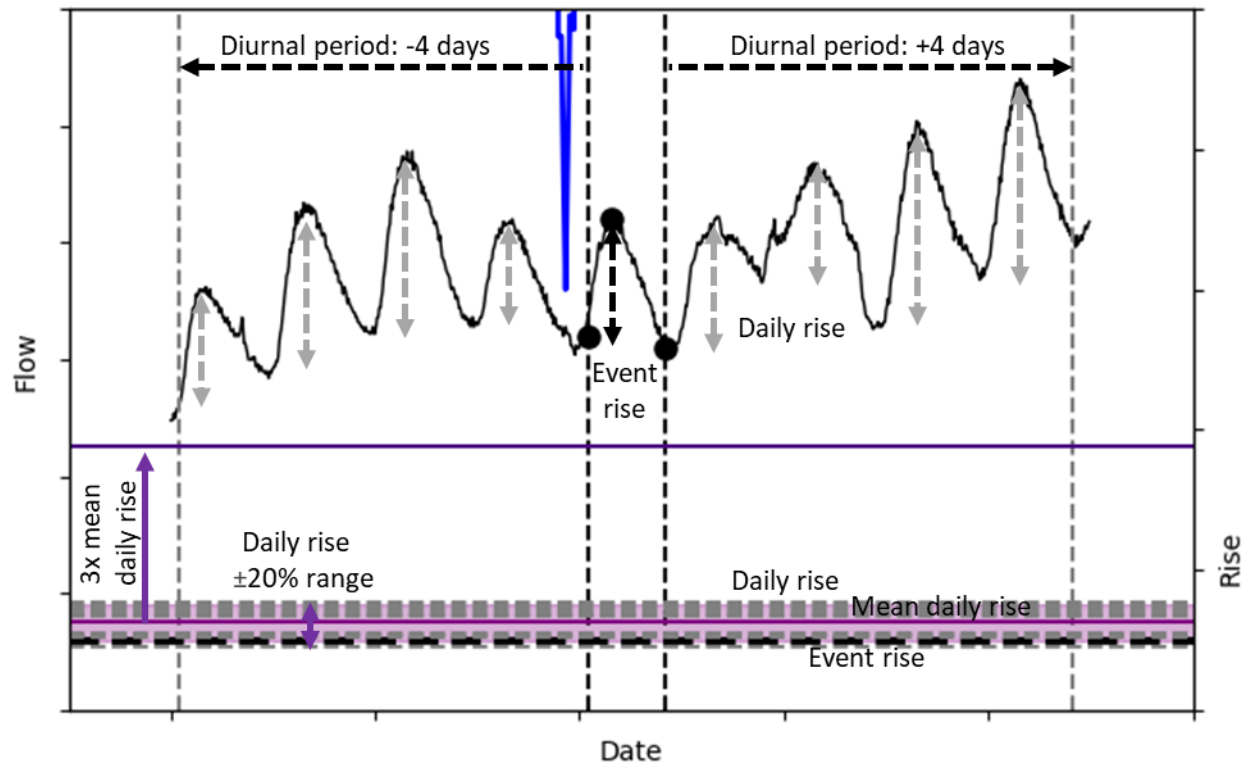


Figure S5: Diurnal cycling flagging method. Shown is an example hydrograph (black), a rainfall event (blue), and paired runoff event start, peak, and end points respectively (black dots). The diurnal cycling period is four days before and after the rainfall-runoff event start and end (vertical dashed grey). The rainfall-runoff event daily range magnitude (black dashed arrow) and the surrounding eight daily ranges (grey dashed arrow) are shown. The magnitude of the rainfall-runoff event range (black dashed horizontal), eight daily ranges (grey dashed horizontal), and mean of the daily ranges (purple) are shown. The $\pm 20\%$ of the mean daily range for determination of within a diurnal cycling period is shown (light purple). The threshold for determination if a rainfall-runoff event is influenced by diurnal cycling is three times the mean daily rise (dark purple). For this example, rainfall-runoff event, it was a diurnal cycling period, and the rainfall-runoff event was influenced by the diurnal cycling.

Table S4: Rainfall-runoff event timing and magnitudes. Including rainfall start, peak 60-minute intensity, and end times, rainfall peak 60-minute intensity, rainfall depth, antecedent precipitation depth, runoff start, peak, and end times and magnitudes, and event volume.

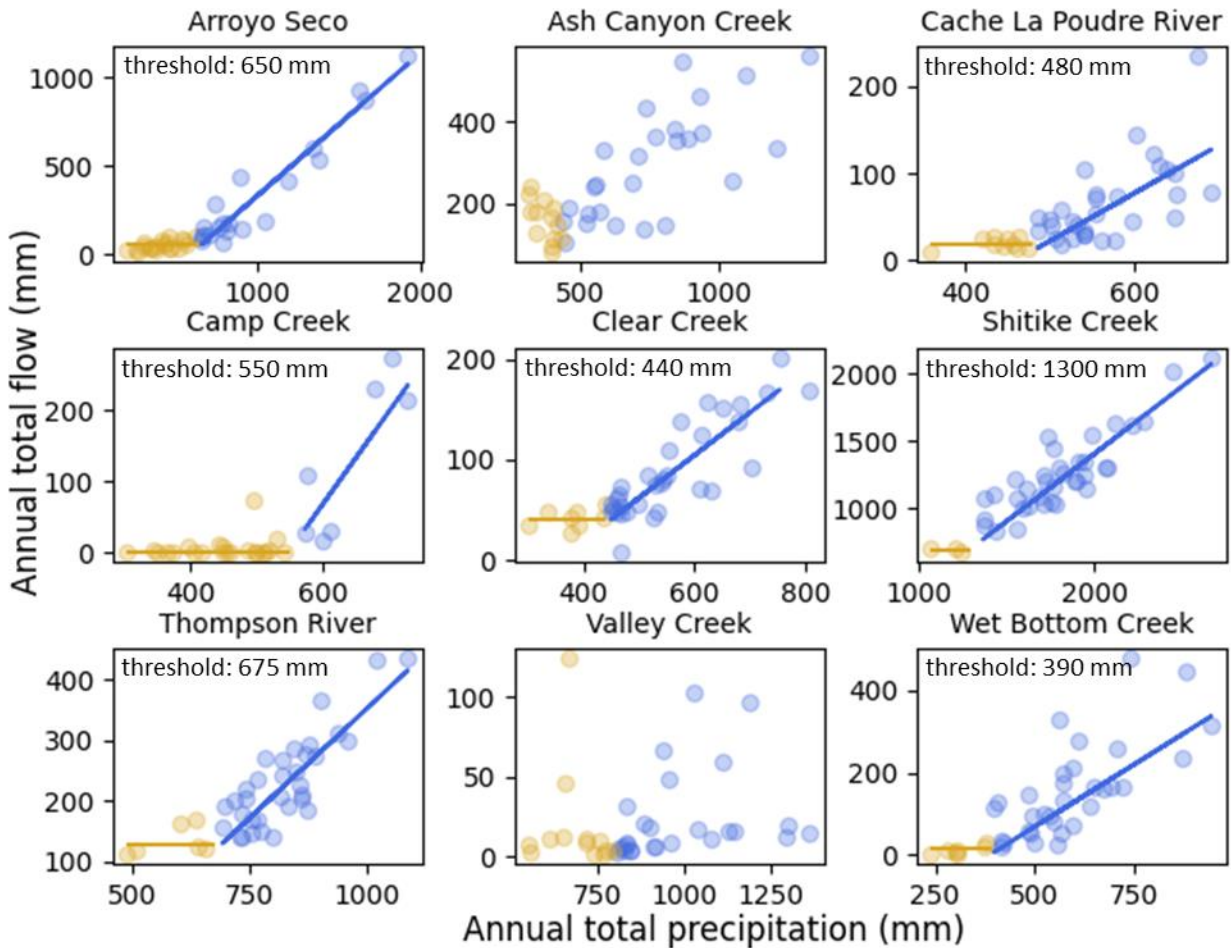
See excel files.

1 **Table S5: RREDI toolkit rainfall-runoff performance results including rainfall-runoff event accuracy, flagging, and retention counts (#) and rates.**

| Watershed | Events pre- flagging (step 2) | Events inspected (#) | Events inspected (%) | Events inspected with 15- minute flow data gaps (issue 1) (%) | Events inspected with diurnal cycling (issue 2) (%) | Events inspected with duplicate events (issue 3) (%) | Events inspected with no end (issue 4) (%) | Event accuracy pre- flagging (step 2) (%) | Events accuracy post- flagging (step 4) (%) | Events retained post- flagging (step 4) (#) | Events retained post- flagging (step 4) (%) |
|---------------------|--|----------------------------|----------------------------|--|---|--|--|--|--|--|--|
| Arroyo Seco | 475 | 40 | 8 | 0 | 0 | 8 | 5 | 88 | 91 | 394 | 83 |
| Ash Canyon Creek | 497 | 48 | 10 | 0 | 2 | 8 | 4 | 75 | 78 | 374 | 75 |
| Cache La Poudre | 1681 | 186 | 11 | 1 | 23 | 6 | 5 | 80 | 93 | 1208 | 72 |
| Camp Creek | 361 | 123 | 34 | 1 | 56 | 2 | 0 | 42 | 88 | 162 | 45 |
| Clear Creek | 1219 | 105 | 9 | 3 | 8 | 9 | 13 | 77 | 89 | 885 | 73 |
| Shitike Creek | 881 | 102 | 12 | 4 | 19 | 0 | 16 | 62 | 93 | 663 | 75 |
| Thompson River | 602 | 75 | 12 | 3 | 4 | 1 | 8 | 67 | 91 | 449 | 75 |
| Valley Creek | 859 | 72 | 8 | 1 | 33 | 1 | 7 | 74 | 91 | 624 | 73 |
| Wet Bottom Creek | 451 | 23 | 5 | 0 | 22 | 0 | 4 | 70 | 100 | 282 | 63 |
| Overall | 7026 | 774 | 11 | 2 | 13 | 4 | 15 | 69 | 90 | 5041 | 72 |

2

S2. Hydrologic control investigation



5 **Figure S6: Wet and dry water year type conditions for all nine study watersheds. Where wet years are blue and**
dry years are orange. A watershed specific precipitation threshold is identified in the watershed average annual
total precipitation and annual total streamflow for the undisturbed years. The ordinary least squares linear
regression trend lines for above (wet, blue) and below (dry, orange) the threshold are shown. For two
watersheds, Ash Canyon Creek and Valley Creek, no threshold behavior was identified, therefore the bottom
10 **third by total annual precipitation years are dry and the top two thirds are wet.**

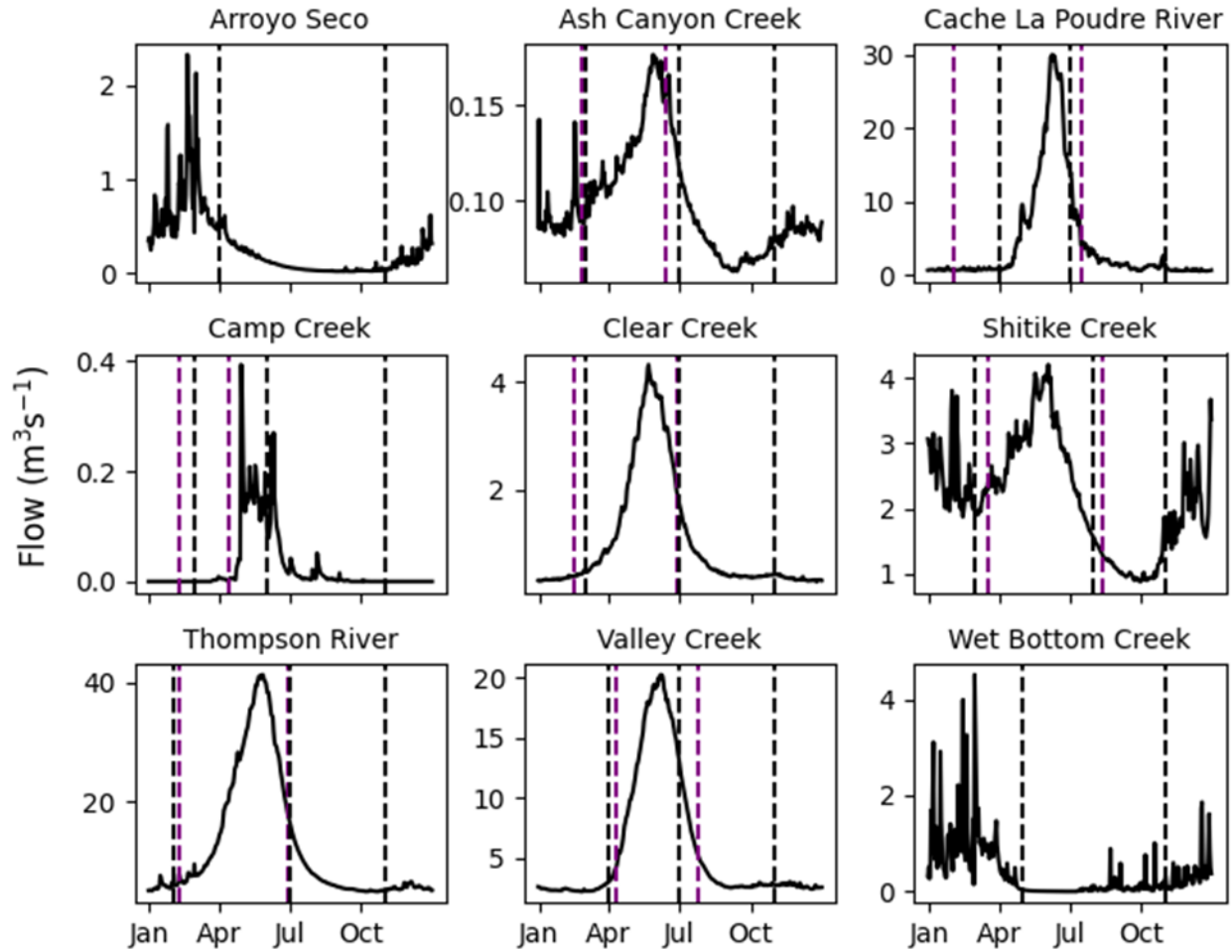


Figure S7: Season condition delineation for all nine study watersheds. Shown is the undisturbed average annual hydrograph. The seasons are delineated (black dashed) as the start of winter, start of melt, and start of summer consecutively for seven snow-dominated watersheds (Ash Canyon Creek, Cache La Poudre River, Camp Creek, Clear Creek, Shitike Creek, Thompson River, Valley Creek). The start of winter and start of summer are delineated consecutively for two non-snow (rain-dominated) watersheds (Arroyo Seco, Wet Bottom Creek). The minimum and maximum snow melt days within the watershed are consecutively shown (purple dashed).

15

Table S6: Percent of rainfall-runoff events assigned to each hydrologic condition for the four hydrologic controls. No melt season was identified for Arroyo Seco and Wet Bottom Creek and only snow-off rainfall-runoff events were included in the antecedent precipitation conditions.

| Watershed | Disturbance | | Water year type | | Season | | | Antecedent precipitation | | |
|-----------------------|-------------|-----------|-----------------|-----|--------|--------|--------|--------------------------|-----|------|
| | Undisturbed | Post-fire | Dry | Wet | Melt | Summer | Winter | None | Low | High |
| | (%) | (%) | (%) | (%) | (%) | (%) | (%) | (%) | (%) | (%) |
| Arroyo Seco | 79 | 21 | 43 | 57 | -- | 23 | 77 | 36 | 34 | 30 |
| Ash Canyon Creek | 70 | 30 | 20 | 80 | 41 | 12 | 47 | 42 | 56 | 2 |
| Cache La Poudre River | 77 | 23 | 27 | 73 | 31 | 47 | 21 | 15 | 78 | 7 |
| Camp Creek | 43 | 57 | 55 | 45 | 60 | 37 | 3 | 5 | 55 | 40 |
| Clear Creek | 80 | 20 | 19 | 81 | 24 | 35 | 41 | 23 | 70 | 7 |
| Shitike Creek | 76 | 24 | 11 | 89 | 51 | 13 | 36 | 29 | 34 | 37 |
| Thompson River | 65 | 35 | 19 | 81 | 47 | 13 | 39 | 28 | 65 | 7 |
| Valley Creek | 72 | 28 | 28 | 72 | 39 | 23 | 38 | 43 | 53 | 4 |
| Wet Bottom Creek | 70 | 30 | 16 | 84 | -- | 31 | 69 | 36 | 35 | 29 |

Table S7: Undisturbed rainfall-runoff events Mann Whitney U Test p-value results for wet and dry conditions for the water year type time-varying hydrologic control. Shading indicates rejection of the null hypothesis at a significance level of 0.05. Glass biserial rank correlation values as an effect size indicator are in parenthesis for significant results.

| Rainfall-runoff event metric | Arroyo Seco | Ash Canyon Creek | Cache La Poudre River | Camp Creek | Clear Creek | Shitike Creek | Thompson River | Valley Creek | Wet Bottom Creek |
|------------------------------|------------------|------------------|-----------------------|------------------|------------------|------------------|------------------|-----------------|------------------|
| volume | <0.001 (0.33) | 0.003 (0.29) | 0.02 (0.10) | 0.005 (0.42) | 0.009 (0.14) | <0.001 (0.26) | 0.02 (0.17) | 0.81 | 0.10 |
| RR | <0.001 (0.34) | <0.001 (0.37) | 0.27 | <0.001 (0.55) | 0.003 (0.16) | 0.02 (0.17) | 0.12 | 0.19 | 0.05 |
| peak | <0.001 (0.44) | 0.006 (0.27) | <0.001 (0.26) | <0.001 (0.59) | <0.001 (0.30) | <0.001 (0.59) | <0.001 (0.34) | 0.002 (0.19) | 0.16 |
| Rise | <0.001 (0.34) | 0.02 (0.23) | 0.004 (0.12) | 0.14 | 0.002 (0.17) | <0.001 (0.32) | 0.02 (0.17) | 0.43 | 0.28 |
| Fall | <0.001 (0.40) | 0.03 (0.21) | <0.001 (0.18) | 0.02 (0.34) | <0.001 (0.19) | <0.001 (0.43) | <0.001 (0.25) | 0.59 | 0.27 |
| Rise_percent | <0.001 (0.24) | 0.07 | 0.14 | 0.37 | 0.64 | 0.007 (0.20) | 0.23 | 0.19 | 0.71 |
| Fall_percent | <0.001 (0.24) | 0.22 | 0.02 (-0.09) | 0.15 | 0.64 | <0.001 (0.26) | 0.10 | 0.04 (-0.13) | 0.57 |
| RiseRate | <0.001 (0.34) | 0.71 | 0.01 (0.11) | 0.35 | 0.02 (0.12) | <0.001 (0.30) | 0.04 (0.15) | 0.70 | 0.65 |
| FallRate | <0.001 (0.45) | 0.10 | <0.001 (0.13) | 0.19 | <0.001 (0.19) | <0.001 (0.45) | 0.011 (0.19) | 0.37 | 0.36 |
| duration | 0.05 | 0.10 | 0.09 | 0.04 (0.30) | 0.56 | 0.24 | 0.08 | 0.50 | 0.07 |
| rising_dur | 0.008 | 0.05 | 0.44 | 0.82 | 0.19 | 0.03 | 0.10 | 0.08 | 0.04 |

| | | | | | | | | | |
|-------------------|------------------|------------------|------------------|------------------|------------------|------------------|------------------|------------------|------|
| | (0.17) | | | | | (0.16) | | (0.29) | |
| falling_dur | 0.48 | 0.99 | 0.20 | 0.012 (0.37) | 0.48 | 0.50 | 0.12 | 0.58 | 0.36 |
| RT1 | 0.005 (0.19) | 0.13 | 0.13 | 0.85 | 0.60 | 0.14 | 0.06 | 0.62 | 0.56 |
| RT2 | 0.50 | 0.41 | 0.02 (-0.10) | 0.53 | 0.34 | 0.006 (-0.21) | 0.2 | 0.013 (-0.15) | 0.23 |
| T2P1 | <0.001 (0.26) | 0.40 | 0.90 | 0.78 | 0.14 | 0.13 | 0.05 | 0.04 (0.13) | 0.09 |
| T2P2 | 0.002 (0.20) | 0.21 | 0.61 | 0.58 | 0.07 | 0.91 | 0.55 | 0.47 | 0.11 |
| T2P3 | 0.93 | 0.20 | 0.36 | 0.48 | 0.06 | 0.30 | 0.62 | 0.39 | 0.63 |
| volume_area | <0.001 (0.33) | 0.003 (0.29) | 0.02 (0.10) | 0.005 (0.42) | 0.009 (0.14) | <0.001 (0.26) | 0.02 (0.17) | 0.81 | 0.10 |
| RR_area | <0.001 (0.34) | <0.001 (0.37) | 0.27 | <0.001 (0.55) | 0.003 (0.16) | 0.02 (0.17) | 0.12 | 0.19 | 0.05 |
| Peak_area | <0.001 (0.44) | 0.006 (0.27) | <0.001 (0.26) | <0.001 (0.59) | <0.001 (0.30) | <0.001 (0.59) | <0.001 (0.34) | 0.00 (0.19) | 0.16 |
| Rise_area | <0.001 (0.34) | 0.02 (0.23) | 0.004 (0.12) | 0.14 | 0.002 (0.17) | <0.001 (0.32) | 0.02 (0.17) | 0.43 | 0.28 |
| Fall_area | <0.001 (0.40) | 0.03 (0.21) | <0.001 (0.18) | 0.02 (0.34) | <0.001 (0.19) | <0.001 (0.43) | <0.001 (0.25) | 0.59 | 0.27 |
| Rise_percent_area | <0.001 (0.24) | 0.07 | 0.14 | 0.37 | 0.64 | 0.007 (0.20) | 0.23 | 0.19 | 0.71 |
| Fall_percent_area | <0.001 (0.24) | 0.22 | 0.02 (-0.09) | 0.15 | 0.64 | <0.001 (0.26) | 0.1 | 0.04 (-0.13) | 0.57 |
| RiseRate_area | <0.001 | 0.02 | 0.00 | 0.14 | 0.002 | <0.001 | 0.02 | 0.43 | 0.28 |

| | | | | | | | | | |
|------------------|------------------|--------|-----------------|-----------------|--------|------------------|--------|------------------|----------------|
| | (0.34) | (0.23) | (-0.12) | | (0.17) | (0.32) | (0.17) | | |
| FallRate_area | <0.001 | 0.03 | <0.001 | 0.02 | <0.001 | <0.001 | <0.001 | 0.59 | 0.27 |
| | (0.40) | (0.21) | (0.18) | (0.34) | (0.19) | (0.43) | (0.25) | | |
| duration_area | 0.05 | 0.10 | 0.09 | 0.04 (0.30) | 0.56 | 0.24 | 0.08 | 0.50 | 0.07 |
| rising_dur_area | 0.008 (0.17) | 0.05 | 0.44 | 0.82 | 0.19 | 0.03 (0.16) | 0.10 | 0.08 | 0.04 (0.29) |
| falling_dur_area | 0.48 | 0.99 | 0.20 | 0.012 (0.37) | 0.48 | 0.50 | 0.12 | 0.58 | 0.36 |
| RT1_area | 0.005 (0.19) | 0.13 | 0.13 | 0.85 | 0.6 | 0.14 | 0.06 | 0.62 | 0.56 |
| RT2_area | 0.50 | 0.41 | 0.02 (-0.10) | 0.53 | 0.34 | 0.006 (-0.21) | 0.20 | 0.013 (-0.15) | 0.23 |
| T2P1_area | <0.001 (0.26) | 0.40 | 0.90 | 0.78 | 0.14 | 0.13 | 0.05 | 0.04 (0.13) | 0.09 |
| T2P2_area | 0.002 (0.20) | 0.21 | 0.61 | 0.58 | 0.07 | 0.91 | 0.55 | 0.47 | 0.11 |
| T2P3_area | 0.93 | 0.20 | 0.36 | 0.48 | 0.06 | 0.30 | 0.62 | 0.39 | 0.63 |

Table S8: Undisturbed rainfall-runoff events Kruskal Wallis Test p-value results for winter, melt, and summer hydrologic conditions for the season time-varying hydrologic control. Shading indicates rejection of the null hypothesis at a significance level of 0.05. In shaded cells, an indicator marks the significantly different condition and no indicator marks all conditions being significantly different from the Dunn Test. Eta squared values as an effect size indicator are in parenthesis for significant results.

| Rainfall-runoff event metric | Arroyo Seco | Ash Canyon Creek | Cache La Poudre River | Camp Creek | Clear Creek | Shitike Creek | Thompson River | Valley Creek | Wet Bottom Creek |
|------------------------------|----------------|------------------|-----------------------|------------|------------------|------------------|------------------|------------------|------------------|
| volume | 0.48 | 0.88 | <0.001 (0.11) | 0.17 | <0.001 * (0.12) | 0.85 | <0.001 (0.078) | <0.001 * (0.14) | 0.008 (0.038) |
| RR | 0.32 | 0.30 | <0.001 (0.074) | 0.43 | <0.001 * (0.087) | <0.001 ^ (0.052) | <0.001 ^ (0.12) | <0.001 (0.20) | 0.06 |
| peak | 0.013 (0.021) | 0.002 ^ (0.058) | <0.001 (0.31) | 0.33 | <0.001 (0.37) | <0.001 (0.099) | <0.001 ^ (0.45) | <0.001 ^ (0.58) | 0.005 (0.043) |
| Rise | 0.05 | 0.96 | <0.001 (0.12) | 0.51 | <0.001 (0.072) | 0.33 | <0.001 ^ (0.093) | <0.001 ^ (0.17) | 0.011 (0.035) |
| Fall | 0.03 (0.016) | 0.89 | <0.001 (0.28) | 0.17 | <0.001 (0.079) | 0.28 | <0.001 (0.18) | <0.001 (0.19) | 0.10 |
| Rise_percent | 0.04 (0.013) | 0.20 | <0.001 (0.017) | 0.98 | <0.001 # (0.034) | 0.001 (0.023) | 0.82 | 0.10 | 0.14 |
| Fall_percent | 0.09 | 0.04 (0.022) | <0.001 (0.12) | 0.05 | <0.001 (0.095) | <0.001 ^ (0.031) | 0.47 | <0.001 # (0.033) | 0.04 (0.020) |
| RiseRate | 0.02 (0.017) | 0.42 | <0.001 (0.12) | 0.34 | <0.001 ^ (0.040) | 0.54 | <0.001 (0.14) | <0.001 ^ (0.16) | 0.27 |
| FallRate | <0.001 (0.041) | 0.78 | <0.001 (0.21) | 0.05 | <0.001 (0.072) | 0.02 # (0.012) | <0.001 ^ (0.13) | <0.001 (0.21) | 0.04 (0.020) |
| duration | 0.15 | 0.35 | 0.04 (0.005) | 0.61 | <0.001 # (0.064) | 0.24 | 0.16 | <0.001 # (0.042) | 0.23 |

| | | | | | | | | | |
|-------------------|------------------|--------------------|-------------------|------|---------------------|---------------------|---------------------|--------------------|-------------------|
| rising_dur | 0.70 | 0.27 | 0.99 | 0.36 | 0.001 * (0.018) | 0.84 | 0.58 | 0.33 | <0.001 (0.071) |
| falling_dur | 0.04 (0.014) | 0.94 | <0.001 (0.029) | 0.92 | <0.001 # (0.10) | 0.002 (0.023) | 0.011 (0.035) | <0.001 (0.13) | 0.26 |
| RT1 | 0.47 | 0.04 (0.024) | 0.87 | 0.19 | <0.001 # (0.039) | <0.001 # (0.029) | 0.005 # (0.042) | 0.02 (0.013) | 0.28 |
| RT2 | 0.45 | 0.28 | 0.65 | 0.9 | 0.014 (0.011) | 0.008 (0.016) | 0.34 | 0.006 (0.019) | 0.36 |
| T2P1 | 0.34 | 0.14 | 0.9 | 0.17 | <0.001 # (0.031) | 0.75 | 0.95 | 0.38 | 0.001 (0.061) |
| T2P2 | 1.0 | 0.19 | 0.95 | 0.47 | <0.001 (0.023) | 0.24 | 0.17 | 0.09 | 0.006 (0.041) |
| T2P3 | 0.005 (0.027) | 0.61 | 0.58 | 0.24 | <0.001 # (0.021) | <0.001 * (0.035) | 0.003 ^ (0.049) | 0.002 (0.025) | 0.40 |
| volume_area | 0.48 | 0.88 | <0.001 (0.11) | 0.17 | <0.001 * (0.12) | 0.85 | <0.001 (0.078) | <0.001 * (0.14) | 0.008 (0.038) |
| RR_area | 0.32 | 0.30 | <0.001 (0.074) | 0.43 | <0.001 * (0.087) | <0.001 ^ (0.052) | <0.001 ^ (0.12) | <0.001 (0.20) | 0.06 |
| Peak_area | 0.013 (0.021) | 0.002 ^ (0.058) | <0.001 (0.31) | 0.33 | <0.001 (0.37) | <0.001 (0.099) | <0.001 ^ (0.45) | <0.001 ^ (0.58) | 0.005 (0.043) |
| Rise_area | 0.05 | 0.96 | <0.001 (0.12) | 0.51 | <0.001 (0.072) | 0.33 | <0.001 ^ (0.093) | <0.001 ^ (0.17) | 0.011 (0.035) |
| Fall_area | 0.02 (0.016) | 0.89 | <0.001 (0.28) | 0.17 | <0.001 (0.079) | 0.28 | <0.001 (0.18) | <0.001 (0.19) | 0.10 |
| Rise_percent_area | 0.04 (0.013) | 0.20 | <0.001 (0.017) | 0.98 | <0.001 # (0.034) | 0.001 (0.023) | 0.82 | 0.10 | 0.14 |

| | | | | | | | | | |
|-----------------------|------------------|-----------------|-------------------|------|---------------------|---------------------|---------------------|---------------------|-------------------|
| Fall_percent_area | 0.09 | 0.04 (0.023) | <0.001 (0.12) | 0.05 | <0.001 (0.095) | <0.001 ^ (0.031) | 0.47 | <0.001 # (0.033) | 0.04 (0.020) |
| RiseRate_area | 0.05 (0.016) | 0.96 | <0.001 (0.12) | 0.51 | <0.001 (0.072) | 0.33 | <0.001 ^ (0.093) | <0.001 ^ (0.17) | 0.011 (0.035) |
| FallRate_area | 0.02 | 0.89 | <0.001 (0.28) | 0.17 | <0.001 (0.079) | 0.28 | <0.001 (0.18) | <0.001 (0.19) | 0.10 |
| duration_area | 0.15 | 0.35 | 0.04 (0.005) | 0.61 | <0.001 # (0.064) | 0.24 | 0.16 | <0.001 # (0.042) | 0.23 |
| rising_duration_area | 0.70 | 0.27 | 0.99 | 0.36 | 0.001 * (0.018) | 0.84 | 0.58 | 0.33 | <0.001 (0.071) |
| falling_duration_area | 0.04 (0.014) | 0.94 | <0.001 (0.029) | 0.92 | <0.001 # (0.10) | 0.002 (0.023) | 0.011 (0.035) | <0.001 (0.13) | 0.26 |
| RT1_area | 0.47 | 0.04 (0.024) | 0.87 | 0.19 | <0.001 # (0.039) | <0.001 # (0.029) | 0.005 # (0.042) | 0.02 (0.013) | 0.28 |
| RT2_area | 0.45 | 0.28 | 0.65 | 0.90 | 0.014 (0.011) | 0.008 (0.016) | 0.34 | 0.006 (0.019) | 0.36 |
| T2P1_area | 0.34 | 0.14 | 0.90 | 0.17 | <0.001 # (0.031) | 0.75 | 0.95 | 0.38 | 0.001 (0.061) |
| T2P2_area | 1.0 | 0.19 | 0.95 | 0.47 | <0.001 (0.023) | 0.24 | 0.17 | 0.09 | 0.006 (0.041) |
| T2P3_area | 0.005 (0.027) | 0.61 | 0.58 | 0.24 | <0.001 # (0.021) | <0.001 * (0.035) | 0.003 ^ (0.049) | 0.002 (0.025) | 0.40 |

Seasons: *Winter, ^Melt, #Summer

Table S9: Undisturbed rainfall-runoff events Kruskal Wallis Test p-value results for none, low, and high hydrologic conditions for the antecedent precipitation time-varying hydrologic control. Shading indicates rejection of the null hypothesis at a significance level of 0.05. In shaded cells, an indicator marks the significantly different condition and no indicator marks all conditions being significantly different from the Dunn Test. Eta squared values as an effect size indicator are in parenthesis for significant results.

| Rainfall-runoff event | Arroyo | Ash Canyon | Cache La Poudre | Camp | Clear | Shitike | Thompson | Valley | Wet Bottom |
|-----------------------|---------------------|------------|-----------------|-------|-------------------|---------|----------------|--------|-----------------|
| metric | Seco | Creek | River | Creek | Creek | Creek | River | Creek | Creek |
| volume | 0.55 | 0.31 | 0.98 | 0.27 | 0.34 | 0.31 | 0.09 | 0.26 | 0.09 |
| RR | 0.42 | 0.15 | 0.83 | 0.30 | 0.04 (0.016) | 0.59 | 0.13 | 0.34 | 0.31 |
| peak | <0.001 + (0.070) | 0.68 | 0.03 (0.008) | 0.71 | 0.05 | 0.26 | 0.06 | 0.20 | 0.87 |
| Rise | 0.33 | 1.00 | 0.83 | 0.78 | 0.34 | 0.17 | 0.09 | 0.51 | 0.18 |
| Fall | <0.001 + (0.055) | 1.00 | 0.02 (0.009) | 0.58 | 0.11 | 0.17 | 0.07 | 0.40 | 0.88 |
| Rise_percent | 0.63 | 0.68 | 0.14 | 0.73 | 0.26 | 0.25 | 0.09 | 0.57 | 0.07 |
| Fall_percent | 0.074 | 0.68 | 0.46 | 0.10 | 0.23 | 0.22 | 0.17 | 0.73 | 0.99 |
| RiseRate | 0.11 | 0.31 | 0.44 | 0.88 | 0.29 | 0.37 | 0.15 | 0.86 | 0.71 |
| FallRate | <0.001 + (0.078) | 0.68 | 0.04 (0.007) | 0.76 | 0.33 | 0.12 | 0.73 | 0.41 | 0.95 |
| duration | 0.29 | 0.54 | 0.33 | 0.15 | 0.15 | 0.70 | 0.17 | 0.10 | 0.11 |
| rising_dur | 0.18 | 0.54 | 0.08 | 0.39 | 0.01 + (0.033) | 0.53 | 0.44 | 0.13 | 0.04 (0.023) |
| falling_dur | 0.51 | 0.68 | 0.91 | 0.30 | 0.84 | 0.37 | 0.04 (0.18) | 0.13 | 0.61 |
| RT1 | 0.33 | 0.84 | 0.02 (0.011) | 0.85 | 0.32 | 0.19 | 0.04 (0.18) | 0.23 | 0.09 |

| | | | | | | | | | |
|-------------------|---------------------|------|-----------------|------|-------------------|------|-----------------|------|-----------------|
| RT2 | 0.52 | 0.41 | 0.34 | 0.58 | 0.10 | 0.37 | 0.027 (0.24) | 0.97 | 0.59 |
| T2P1 | 0.08 | 0.54 | 0.03 (0.008) | 0.54 | 0.01 (0.036) | 0.93 | 0.73 | 0.09 | 0.02 (0.038) |
| T2P2 | 0.22 | 0.41 | 0.04 (0.006) | 0.71 | <0.001 (0.041) | 0.47 | 0.17 | 0.10 | 0.03 (0.029) |
| T2P3 | 0.36 | 0.22 | 0.04 (0.007) | 1.00 | 0.01 (0.040) | 0.12 | 0.13 | 0.91 | 0.46 |
| volume_area | 0.55 | 0.31 | 0.98 | 0.27 | 0.34 | 0.31 | 0.09 | 0.26 | 0.09 |
| RR_area | 0.42 | 0.15 | 0.83 | 0.30 | 0.04 (0.016) | 0.59 | 0.13 | 0.34 | 0.31 |
| Peak_area | <0.001 + (0.070) | 0.68 | 0.03 (0.008) | 0.71 | 0.05 (0.041) | 0.26 | 0.06 | 0.20 | 0.87 |
| Rise_area | 0.33 | 1.00 | 0.83 | 0.78 | 0.34 | 0.17 | 0.09 | 0.51 | 0.18 |
| Fall_area | <0.001 + (0.055) | 1.00 | 0.02 (0.009) | 0.58 | 0.11 | 0.17 | 0.07 | 0.40 | 0.88 |
| Rise_percent_area | 0.63 | 0.68 | 0.14 | 0.73 | 0.26 | 0.25 | 0.09 | 0.57 | 0.07 |
| Fall_percent_area | 0.07 | 0.68 | 0.46 | 0.10 | 0.23 | 0.22 | 0.17 | 0.73 | 0.98 |
| RiseRate_area | 0.33 | 1.00 | 0.83 | 0.78 | 0.34 | 0.17 | 0.09 | 0.51 | 0.18 |
| FallRate_area | <0.001 + (0.055) | 1.00 | 0.02 (0.009) | 0.58 | 0.11 | 0.17 | 0.07 | 0.40 | 0.88 |
| duration_area | 0.29 | 0.54 | 0.33 | 0.15 | 0.15 | 0.70 | 0.17 | 0.10 | 0.11 |
| rising_dur_area | 0.18 | 0.54 | 0.08 | 0.39 | 0.01 + (0.033) | 0.53 | 0.44 | 0.13 | 0.04 (0.023) |
| falling_dur_area | 0.51 | 0.68 | 0.91 | 0.30 | 0.84 | 0.37 | 0.04 (0.18) | 0.13 | 0.61 |
| RT1_area | 0.33 | 0.84 | 0.02 | 0.85 | 0.32 | 0.19 | 0.04 | 0.23 | 0.09 |

| | | | | | | | | | |
|--|------|------|---------|------|----------|------|--------|------|---------|
| | | | (0.011) | | | | (0.18) | | |
| | | | | | | | 0.03 | | |
| RT2_area | 0.52 | 0.41 | 0.34 | 0.58 | 0.10 | 0.37 | (0.24) | 0.97 | 0.59 |
| | | | 0.03 | | 0.01 + | | | | 0.02 |
| T2P1_area | 0.08 | 0.54 | (0.008) | 0.54 | (0.036) | 0.93 | 0.73 | 0.09 | (0.038) |
| | | | 0.04 | | <0.001 + | | | | 0.03 |
| T2P2_area | 0.22 | 0.41 | (0.006) | 0.71 | (0.041) | 0.47 | 0.17 | 0.10 | (0.029) |
| | | | 0.04 | | 0.01 + | | | | |
| T2P3_area | 0.36 | 0.22 | (0.007) | 1.00 | (0.040) | 0.12 | 0.13 | 0.91 | 0.46 |
| Antecedent precipitation: &None, ~Low, +High | | | | | | | | | |

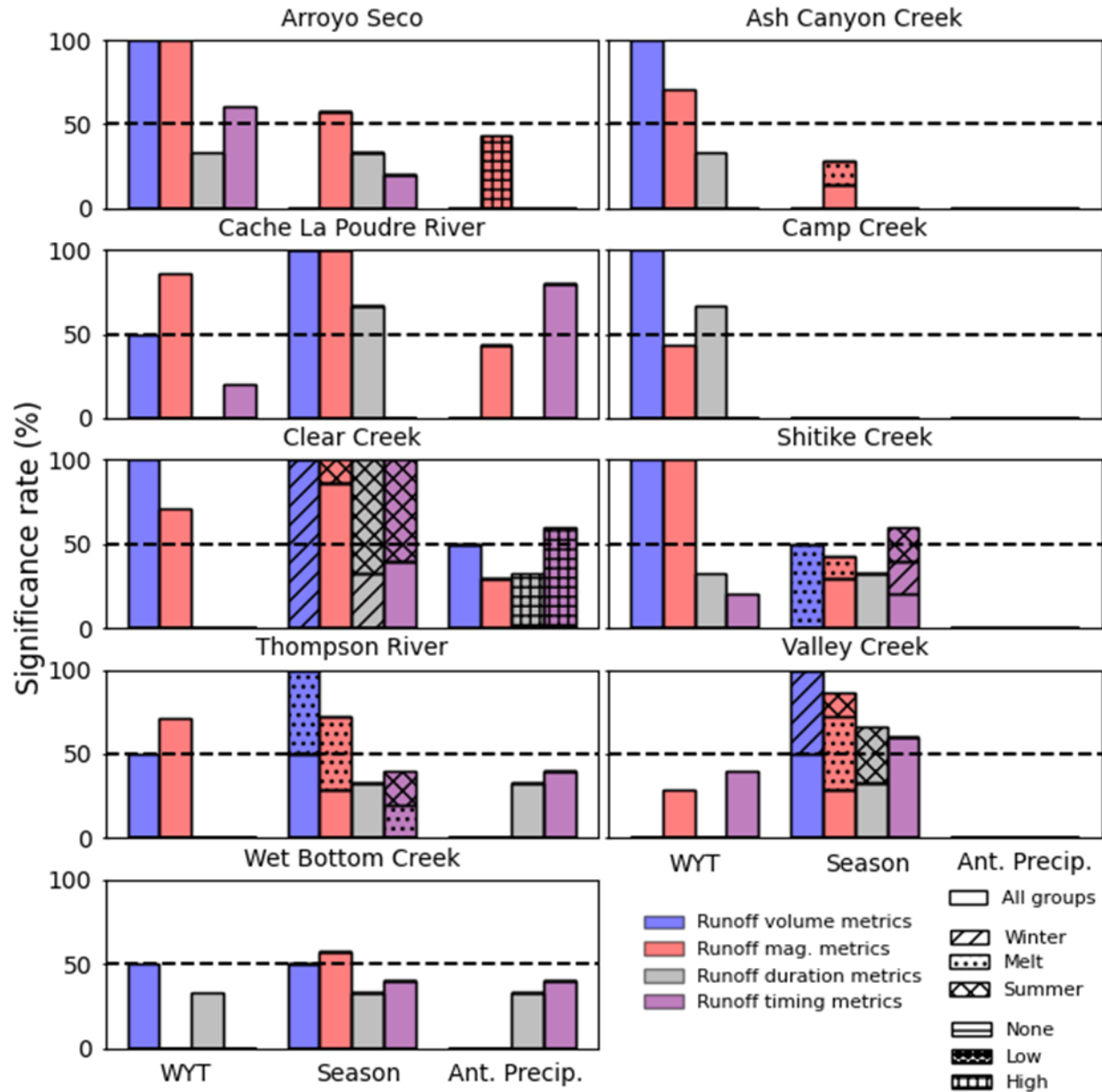


Figure S8: Event runoff metric group significance summary rates for statistical test results for area-normalized metrics. Individual plots for each study watershed. Shown are the average significance rates within the four rainfall-runoff metric groups including runoff volume metrics (blue), runoff magnitude metrics (red), runoff duration metrics (grey), and rainfall-runoff timing metrics (purple). Bars are grouped by time-varying hydrologic control (WYT, season, antecedent precipitation). The WYT group shows results of the Mann Whitney U Test. The season and antecedent precipitation groups show results from the Kruskal Wallis Test. The hatching within the bars represents statistically different individual hydrologic conditions from the Dunn Test where no hatching indicates all hydrologic conditions were statistically different. The 50% rate is

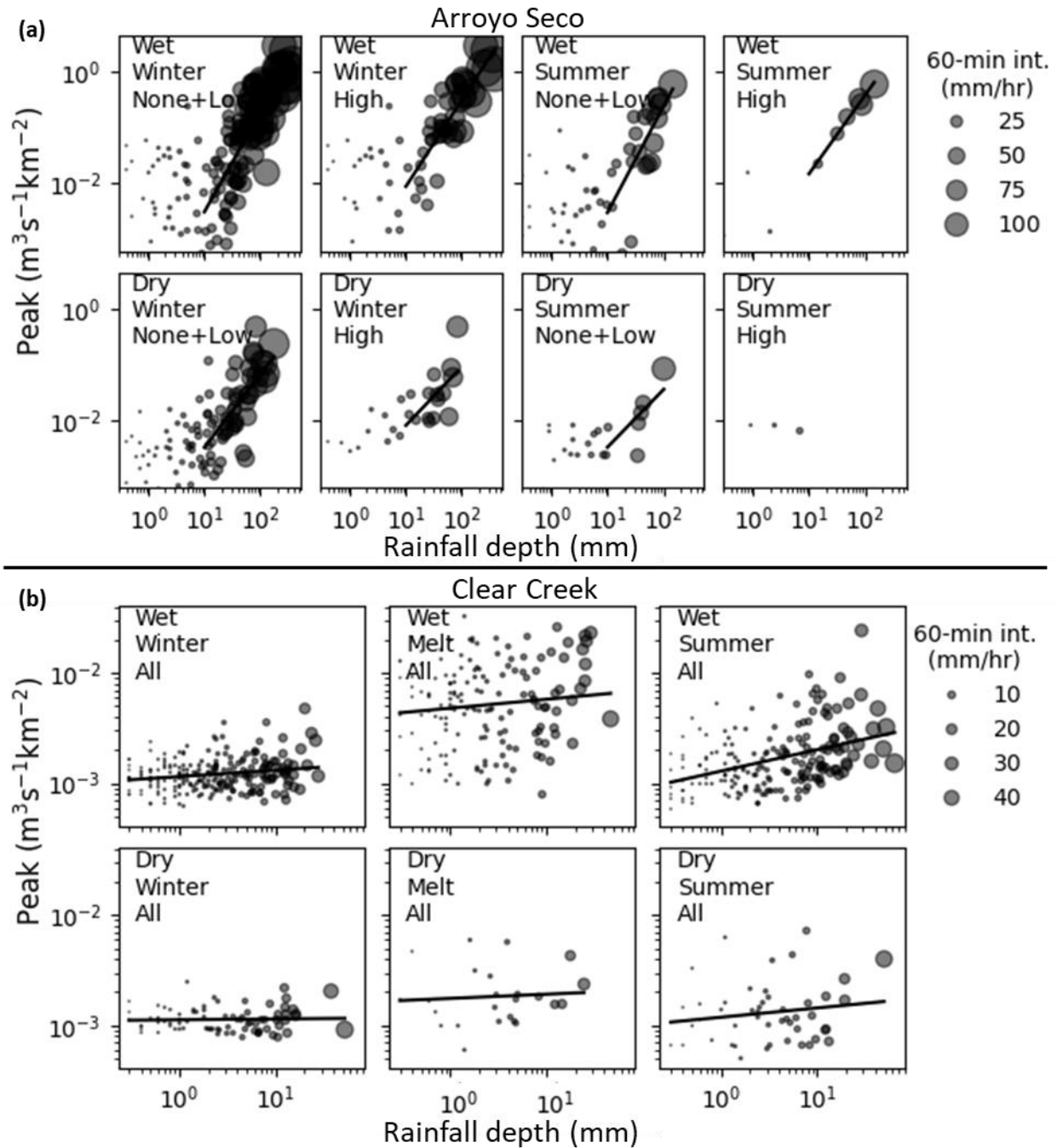


Figure S9: Hydrologic condition permutations for Arroyo Seco (a) and Clear Creek (b) for the rainfall depth (mm) and runoff peak ($\text{m}^3 \text{s}^{-1} \text{km}^{-2}$) relationship. Where undisturbed rainfall-runoff events and the permutation power trend are shown. Rainfall-runoff events are sized by 60-minute peak rainfall intensity (mm hr^{-1}).

50

Table S10: Power trend slope and intercepts in log-log space for significant condition groups for Arroyo Seco and Clear Creek for the rainfall depth (mm) and runoff peak ($\text{m}^3 \text{s}^{-1} \text{km}^{-2}$) relationship.

| Group | Slope | Intercept |
|---------------|-------|-----------|
| Arroyo Seco | | |
| All | 1.74 | -9.89 |
| Wet, None+Low | 1.88 | -10.63 |
| Wet, High | 1.54 | -8.20 |
| Dry | 1.29 | -8.69 |
| Clear Creek | | |
| All | 0.080 | -6.39 |
| Summer | 0.18 | -6.67 |
| Winter | 0.041 | -6.77 |
| Wet, Melt | 0.081 | -5.33 |
| Dry, Melt | 0.038 | -6.34 |

55 Table S11: Percent of post-fire rainfall-runoff events above the undisturbed trend line and plus one standard deviation for grouped rainfall-runoff events in Arroyo Seco and Clear Creek. Shading indicates percent at or above expected (50% for trend line, 16% for plus one standard deviation).

| Year since fire | | All | 0 | 1 | 2 | 3 | 4 | 5 | 6 |
|-----------------|------------------------|-----|----|-----|----|----|-----|----|-----|
| Arroyo Seco | | | | | | | | | |
| Wet, None + Low | Above trend line (%) | 93 | 86 | 100 | -- | -- | -- | -- | -- |
| | Above +1 std. dev. (%) | 57 | 71 | 43 | -- | -- | -- | -- | -- |
| Wet, High | Above trend line (%) | 67 | 75 | 50 | -- | -- | -- | -- | -- |
| | Above +1 std. dev. (%) | 33 | 50 | 0 | -- | -- | -- | -- | -- |
| Dry | Above trend line (%) | 56 | -- | -- | 67 | 50 | 50 | 33 | 100 |
| | Above +1 std. dev. (%) | 7 | -- | -- | 0 | 0 | 0 | 11 | 25 |
| Clear Creek | | | | | | | | | |
| Summer | Above trend line (%) | 74 | 56 | 100 | 71 | 67 | 57 | 67 | 71 |
| | Above +1 std. dev. (%) | 26 | 44 | 47 | 6 | 8 | 29 | 67 | 14 |
| Winter | Above trend line (%) | 40 | 0 | 50 | 17 | 33 | 20 | 50 | 70 |
| | Above +1 std. dev. (%) | 10 | 0 | 0 | 0 | 22 | 0 | 0 | 30 |
| Wet, Melt | Above trend line (%) | 56 | 82 | 33 | 0 | 0 | -- | 50 | 100 |
| | Above +1 std. dev. (%) | 20 | 45 | 0 | 0 | 0 | -- | 0 | 0 |
| Dry, Melt | Above trend line (%) | 100 | -- | -- | -- | -- | 100 | -- | -- |
| | Above +1 std. dev. (%) | 43 | -- | -- | -- | -- | 43 | -- | -- |

References

- 60 Canham, H. A., and Lane, B.: Rainfall-runoff event detection and identification (RREDI) toolkit, Hydroshare [code] <https://www.hydroshare.org/resource/797fe26dfefb4d658b8f8bc898b320de/>, 2022.
- Chapman, T. G., and Maxwell, A. I.: Baseflow Separation—Comparison of Numerical Methods with Tracer Experiments, Hydrology and Water Resources Symposium 1996: Water and the Environment; Preprints of Papers, Institute of Engineers, Australia, 539–545, <https://doi.org/10.3316/informit.360361071346753>, 1996.
- 65 Eckhardt, K.: How to construct recursive digital filters for baseflow separation, *Hydrol. Process.*, 19(2), 507–515, <https://doi.org/10.1002/hyp.5675>, 2005.
- Fall, G., Kitzmiller D., Pavlovic S., Zhang Z., Patrick, N., St. Laurent, M., Trypaluk, C., Wu, W., Miller, D.: The Office of Water Prediction’s Analysis of Record for Calibration, version 1.1: Dataset description and precipitation evaluation, *J. Am. Water Resour. As.*, 59(6), 1246–1272, [https://doi.org/10.1111/1752-](https://doi.org/10.1111/1752-1688.13143)
- 70 1688.13143, 2023.
- Lane, B. A., Sandoval-Solis, S., Stein, E. D., Yarnell, S. M., Pasternack, G. B., and Dahlke, H. E: Beyond Metrics? The Role of Hydrologic Baseline Archetypes in Environmental Water Management, *Environ. Manag.*, 62(4), 678–693. <https://doi.org/10.1007/s00267-018-1077-7>, 2018.
- Patterson, N. K., Lane, B. A., Sandoval-Solis, S., Pasternack, G. B., Yarnell, S. M., and Qiu, Y.: A hydrologic
- 75 feature detection algorithm to quantify seasonal components of flow regimes, *J. Hydrol.*, 585, 124787, <https://doi.org/10.1016/j.jhydrol.2020.124787>, 2020.